ChemPubSoc Europe

DOI: 10.1002/chem.201402916

CHEMISTRY
A European Journal
Full Paper

Hydrogels

Phosphate-Triggered Self-Assembly of *N*-[(Uracil-5-yl)methyl]urea: A Minimalistic Urea-Derived Hydrogelator

Alexander J. Kleinsmann, Nicole M. Weckenmann, and Boris J. Nachtsheim*[a]

Abstract: *N*-[(Uracil-5-yl)methyl]urea is reported as a minimalistic low-molecular-weight hydrogelator (LMWHG). The unusual phosphate-induced assembly of this compound has been thoroughly investigated by IR, UV/Vis, and NMR spectroscopy, electron microscopy, and rheological experiments. This rare example of an anion-triggered urea-based LMWHG is the first example of a pyrimidine- and urea-containing molecule that can be forced into self-assembly in aqueous solution without additional aromatic or lipophilic groups. The gelator/phosphate ratio within the hydrogel was successfully determined by ^{31}P MAS NMR spectroscopy. The hydrogel exhibits a very fast and repeatable self-healing property, and remarkable *G*′ values. The viscoelastic properties of the hydrogel can easily be tuned by variation of the phosphate ratio.

Introduction

Gels are colloidal mixtures of self-assembled low-molecular-weight compounds (low-molecular-weight gelators, LMWGs) or polymers that are able to retain given solvent molecules by physical effects such as surface tension.[1,2] Gels based on LMWGs are constructed of individual molecules organized through a self-complementary network of interactions such as hydrogen bonding, which enables them to assemble into extended fibers and grants the corresponding gels particular advantages over covalently linked chemical gels: They are thermoreversible and their physical properties can be easily tuned by external stimuli such as temperature, anions,[1,3] pH,[4] sonication,[5] or UV light.[6] Therefore supramolecular gels have recently received attention as versatile media for creating and controlling attractive functions.[7]

Gelators that are capable of solidifying water to form the so-called hydrogels are of particular interest because these innovative materials play a vital role in biomedical applications such as tissue engineering, retained drug delivery systems, and implants.[8] The general structural requisites for low-molecular-weight hydrogelators (LMWHGs) are appropriate hydrogen-bond donor and acceptor moieties, which are responsible for conferring sufficient solubility and strong self-assembly.[9] However, particularly in water, intermolecular hydrogen-bonding networks are in general not sufficient to render a molecule an efficient hydrogelator: Additional π–π stacking, metal coordination, or van der Waals interactions are necessary.

Although it has so far been impossible to rationally predict the gelation ability of a particular compound, ureas, nucleobases, and peptides, or combinations thereof, have been investigated intensively in this regard and have been found to show excellent hydrogelating properties because they are all capable of excessive hydrogen bonding and therefore prone to self-assembly. However, the hydrogelation of urea (Figure 1a)[10–12,15] and pyrimidine derivatives (Figure 1b) has only been achieved so far by the inclusion of aromatic or lipophilic groups to assist the formation of the hydrogen-bonding network in aqueous solutions through π–π and/or van der Waals interactions.[8e,13,14,16]

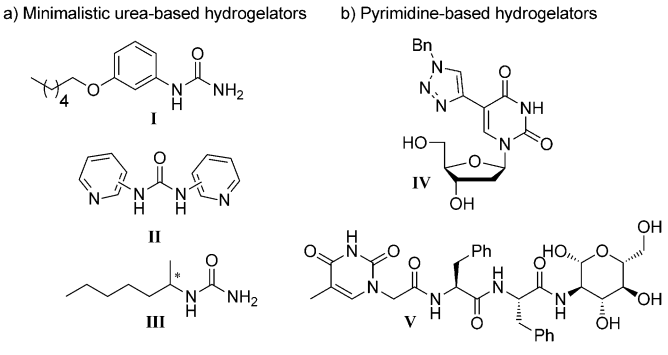

Figure 1. Typical examples of urea (**I**,[10] **II**,[11] **III**[12]) and nucleobase (**IV**,[13] **V**[14]) containing hydrogelators.

Our group is highly interested in minimalistic peptide- and nucleobase-based LMWHGs,[17] and within this context we now wish to introduce *N*-[(uracil-5-yl)methyl]urea (UMU, **2**; Figure 2) as the lowest-molecular-weight nucleobase-derived hydrogelator to be described so far. We assumed that the combination of both a urea and a pyrimidine motif would lead to a simple

[a] *A. J. Kleinsmann, N. M. Weckenmann, Prof. B. J. Nachtsheim*
Institut für Organische Chemie, Eberhard Karls Universität Tübingen
Auf der Morgenstelle 18, 72076 Tübingen (Germany)
E-mail: boris.nachtsheim@uni-tuebingen.de

Supporting information for this article is available on the WWW under http://dx.doi.org/10.1002/chem.201402916.

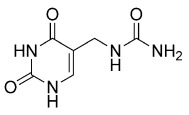

2 (UMU)

Figure 2. Chemical structure of *N*-[(uracil-5-yl)methyl]urea (UMU, **2**).

and effective hydrogelator based on natural, cheap, and readily available building blocks. In this study we have found that **2** is not only a remarkable small-nucleobase-comprising hydrogelator, but also a very rare example of a urea-containing LMWHG, which can be forced into self-assembly exclusively by the addition of phosphate anions, which usually breaks the urea α-tape motif responsible for supramolecular aggregation.[1,15f,m,18,19]

Results and Discussion

Synthesis of *N*-[(uracil-5-yl)methyl]urea 2

N-[(uracil-5-yl)methyl]urea (UMU, **2**) was obtained in a straightforward two-step synthesis from uracil. The literature-known synthesis was greatly improved by direct condensation of 5-hydroxymethyluracil (**1**) with urea under acidic conditions, which gave **2** in a good isolated yield of 82% (Scheme 1).[20,21] This new synthesis was achieved in water in a fewer number of steps and in higher yield than that previously reported. Furthermore, the reactants are naturally available compounds, UMU precipitates as the only product, and can be used without further purification.

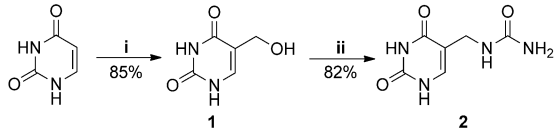

Scheme 1. Improved synthesis of *N*-[(uracil-5-yl)methyl]urea (**2**). Reagents and conditions: i) paraformaldehyde, KOH, H_2O, 55 °C, 72 h; ii) urea, HCl_{aq}, H_2O, 80 °C, 4 h.

Initial hydrogelation studies

The hydrogelation of **2** was studied by using a simple "upside-down tube" test. Initially, a defined amount (5 wt%) of **2** was heated until boiling at pH 7 in pure water. We found that **2** is insoluble at neutral pH and therefore decided to test the hydrogelation at pH 10 because **2** should deprotonate at this pH to form a more soluble monoanionic species. Even though **2** completely dissolved in boiling water at pH 10, no hydrogelation was observed after rapid cooling in an ice bath. Instead, **2** precipitated again as a white solid (Table 1, entry 1). A white precipitate was also formed in aqueous sulfate-, acetate-, carbonate-, and chloride-containing buffer solutions at pH 10 (Table 1, entries 2–5). The finding that no hydrogelation was observed in aqueous buffer solutions was not surprising because strongly coordinating anions usually prevent or at least weaken the self-assembled state by disturbing the urea α-tape motif, a key interaction that has been described extensively in the aggregation of other urea-based hydrogelators.[1,15h,m,19,22]

Table 1. Gelation studies of **2** (5 wt%) in water and aqueous buffers.

Entry	Solvent, aq. buffer[a,b]	pH 7	pH 10[c]
1	H_2O	insoluble	P[b]
2	$Na_2SO_4/NaHSO_4$	insoluble	P[b]
3	NaOAc/HOAc	insoluble	P[b]
4	$Na_2CO_3/NaHCO_3$	insoluble[d]	P
5	NaCl	insoluble	P[b]
6	Na_3PO_4/NaH_2PO_4	insoluble	GEL
7	K_3PO_4/KH_2PO_4	insoluble	P

[a] Buffer concentration = 1.0 M. [b] The pH was additionally adjusted with aq. NaOH. [c] P = precipitation; GEL = hydrogel formation. [d] The pH was additionally adjusted with aq. HCl.

When we repeated the same experiment with 1 M sodium phosphate buffer, we were delighted to observe the formation of a turbid hydrogel (Table 1, entry 6 and Figure 3, left). Reduction of the hydrogelator concentration from 5 to 2.5 wt% resulted in the formation of an opaque hydrogel (Figure 3, right). On the basis of this observation, the molecular assembly of **2** must be significantly different from most of urea-based gels reported in the literature, which often exhibit urea α-tapes. These structural motifs are usually disrupted by phosphate anions and therefore this is a very rare example of phosphate-induced self-assembly of a urea-based hydrogelator.[15f] However, it is worth mentioning that the cation must also play a crucial role in the self-assembly process because changing the buffer from sodium to potassium phosphate again disrupted gel formation (Table 1, entry 7).

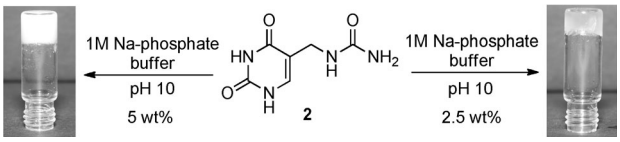

Figure 3. Macroscopic appearance of hydrogels containing **2** at different concentrations in 1.0 M sodium phosphate buffer at pH 10.

Detailed studies on the hydrogelation ability of this system were carried out by using different phosphate/gelator ratios at constant pH. Figure 4 shows the minimum gelator concentration (MGC) of **2** as a function of phosphate equivalents added. With mixtures containing less than 1 equiv of phosphate or below a gelator concentration of 1.0 wt%, no hydrogel formation was observed. A blend with the minimal amount of phosphate exhibited a relatively high MGC of 5 wt%, which decreased with increasing amounts of phosphate. By adding 4 equiv of phosphate, the MGC dropped significantly to 1.5 wt%. Increasing the phosphate/gelator ratio further to 6:1 had no significant impact on the MGC. However, by adding 8 equiv of phosphate, a slight decrease in MGC to a minimal value of 1 wt% was observed. Addition of more than 8 equiv of phosphate did not have any further impact on the MGC.

The gel–sol transition temperature was determined by rheological temperature sweep experiments (Figure 5). We found

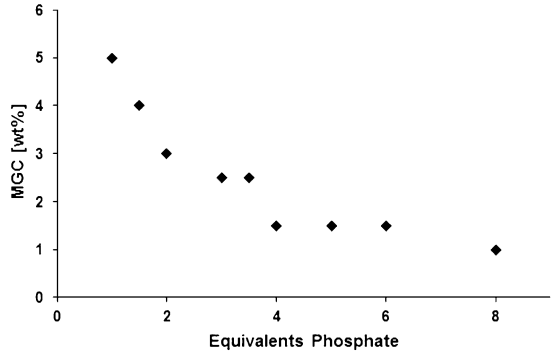

Figure 4. MGC of **2** at pH 10 with different ratios of sodium phosphate.

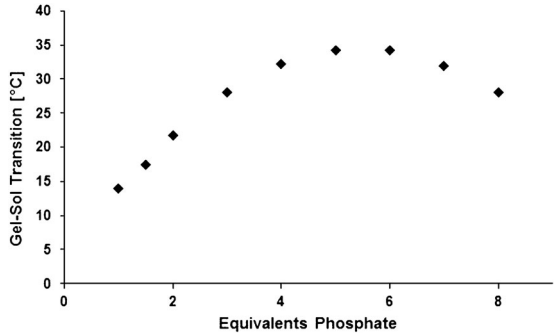

Figure 5. Gel–sol transition temperature of **2** (5 wt%, pH 10) at different ratios of phosphate.

that the thermal stability of the hydrogel increases with increasing phosphate/**2** ratio until 5 equiv of phosphate had been added. However, further addition of phosphate reduced the thermal stability again.

Electron microscopy

The morphology of the hydrogel was determined by scanning electron microscopy (SEM) and transmission electron microscopy (TEM). The macroscopic morphology is roughly visible without magnification, showing a parallel sheet structure (Figure 6A). Higher magnifications revealed dense lamellae with a thickness of approximately 1–2 μm (Figure 6B,C) and a low degree of cross-linking between the lamellae. A considerable number of amorphous spheres in the range of 5–10 μm were equally distributed over the sample (Figure 6A,B). Although the lamellae appear to be rather robust and dense, TEM analysis revealed their highly porous and sponge-like interior, with pores as small as 10 nm in diameter (Figure 6D).

Surprisingly, higher magnifications did not show clearly defined nanofibers, as in most supramolecular hydrogels.[8e,9,23] However, other hydrogels containing high amounts of salt additives showing particle-based and porous sponge-like morphologies without observable nanofibers have already been reported.[15f,24]

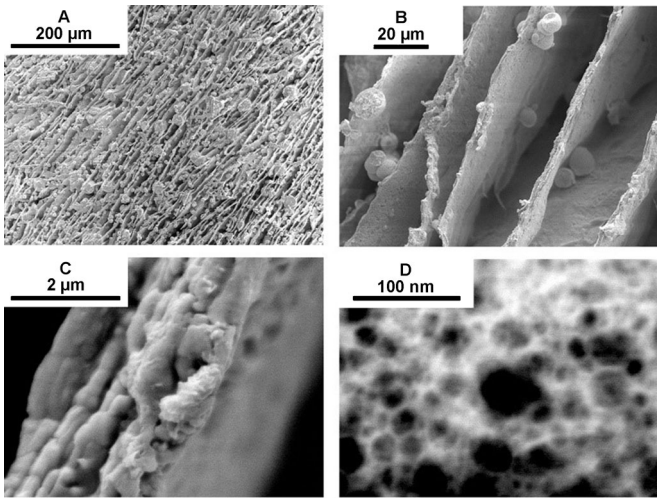

Figure 6. A–C) SEM and D) TEM images of the xerogel of **2** (5 wt% of **2** in 1.0 M sodium phosphate) at pH 10.

NMR studies

NMR titration experiments were conducted to investigate the coordination affinity of phosphate to **2** and to verify the hydrogelator/anion stoichiometry. ^{13}C NMR titration studies with sodium phosphate were undertaken in D_2O at pH 10, close to the conditions of gelation. Strong shifts were observed for the uracil carbons C-2, C-4, and C-6 (Figure 7), which suggests

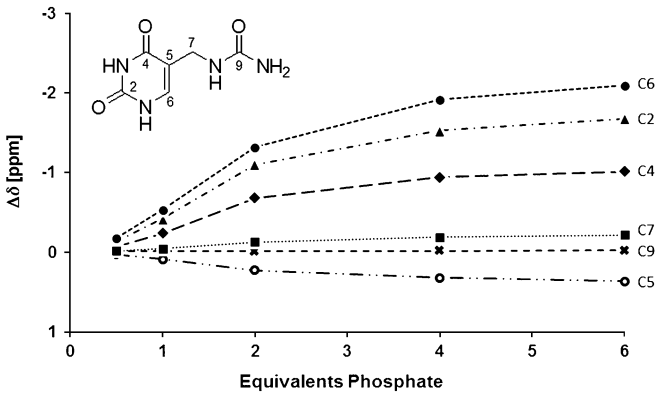

Figure 7. ^{13}C NMR titration experiment of **2** with sodium phosphate at pH 10 in D_2O.

a strong coordination of phosphate to the uracil ring, a shift of the tautomer equilibrium (see the UV/Vis spectroscopy section), or both. The most significant shifts were observed up to the addition of 4 equiv of phosphate. A saturation effect can be observed at higher concentrations of phosphate, with no notable increase in the shifts detected.

The ^1H NMR shifts of **2** in [D_6]DMSO were also plotted against equivalents of monobasic tetrabutylammonium phosphate added (Figure 8). Two urea signals, H8 and H10, as well as the uracil signal of H6 were observed. All the signals were shifted downfield upon addition of phosphate. However, the strongest downfield shift of more than 1.2 ppm was observed

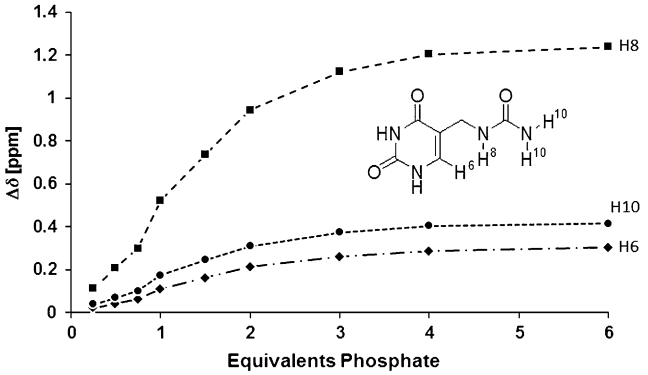

Figure 8. ^{1}H NMR titration experiment of **2** with tetrabutylammonium dihydrogen phosphate in [D_6]DMSO.

for 8-H, again with a saturation effect in excess of 4 equiv of phosphate, which confirms the former trend.

For both titration experiments, a clear step-like increase in the shifts occurred when 1 equiv phosphate was added, which was previously described as the minimal amount of phosphate additive needed to obtain a hydrogel. This result again implies that a sudden self-assembly process is triggered at that particular phosphate ratio.

^{31}P MAS NMR titration experiments of hydrogels containing **2** and different molar fractions of phosphate were performed to quantify the phosphate/gelator stoichiometry within the gel through a Job plot analysis. The spectra show two different phosphorus states (Figure 9): A sharp signal at 2.84 ppm represents the amount of free phosphate in solution and a broadened signal with spinning sidebands at about 0.40 ppm reflect the phosphate incorporated into the hydrogel network.

Figure 10 displays the corresponding Job plot analysis. The molarity of phosphate solidified within the hydrogel was determined by integration of the broadened signals. A maximum was observed at a mole fraction χ(phosphate) of 0.6, which correlates to a **2**/phosphate ratio of 1:1.5 within the hydrogel network. This result confirms that the phosphate anion not only coordinates to the urea groups and leads to urea–phosphate–urea dimers, but also plays a vital role in the self-assembly process, presumably by additional coordination to the uracil moieties, as already implied by the results of the ^{13}C NMR titration experiments.

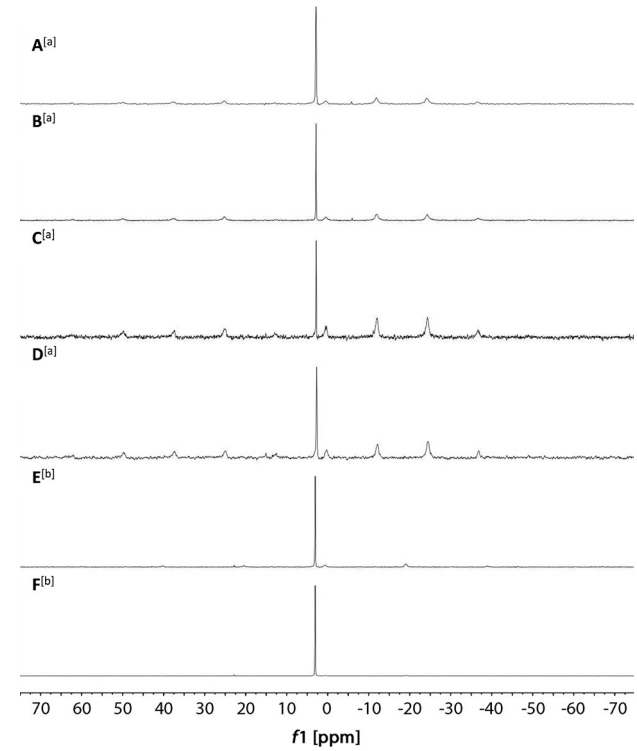

Figure 9. ^{31}P MAS NMR titration experiments of hydrogels containing **2** at pH 10 in D_2O at different molar fractions of sodium phosphate: A) $\chi = 0.47$, B) $\chi = 0.50$, C) $\chi = 0.60$, D) $\chi = 0.67$, E) $\chi = 0.8$, and F) $\chi = 0.86$. [a] 2.5 kHz spinning frequency. [b] 4.0 kHz spinning frequency.

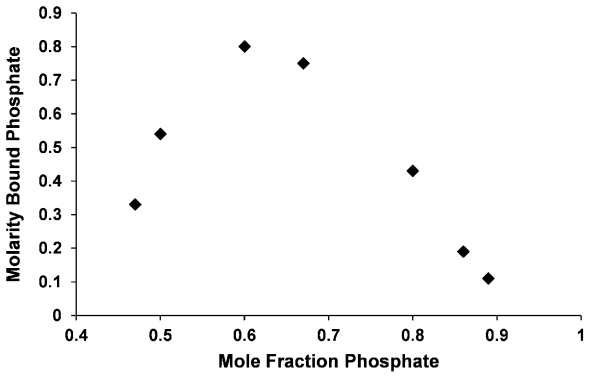

Figure 10. Job plot analysis of **2**/phosphate hydrogels at pH 10.

FTIR spectroscopy

FTIR spectroscopy is a powerful tool for the structural analysis of a hydrogel network, and has been extensively used to investigate gelation because the IR spectrum of the gel state can easily be compared with solution and solid states.

The FTIR spectrum of a 1.0 wt% supersaturated solution of **2** in 1.0 M sodium phosphate buffer at pH 10 (Figure 11, dotted line) shows absorption bands at $\tilde{\nu} = 3314$ (ν_{N-H}), 1632 ($\nu_{C=O}$), 1070 (ν_{P-O}), and 982 cm^{-1} (ν_{P-O}).[25] Subsequent cooling of this solution for 10 min in an ice bath resulted in a metastable hydrogel, the IR spectrum of which was instantly recorded. The spectrum of the gel reveals explicit changes (continuous line). The IR of the hydrogel shows that the characteristic NH stretching band shifts from 3314 to 3146 cm^{-1} due to strong hydrogen bonding with C=O groups during the self-assembly,[26] and the carbonyl stretching vibration band observed in solution at 1632 cm^{-1} shifts to 1675 cm^{-1}, which can also be attributed to hydrogen-bonding interactions with the uracil N–H protons.[26]

Furthermore, a strong increase in the intensities of the phosphate bands at 1070 and 982 cm^{-1} due to rigidification of the phosphate clearly confirms the incorporation of phosphate into the supramolecular assembly. Comparison of the IR spectra of supersaturated solutions of **2** in sodium and potassium

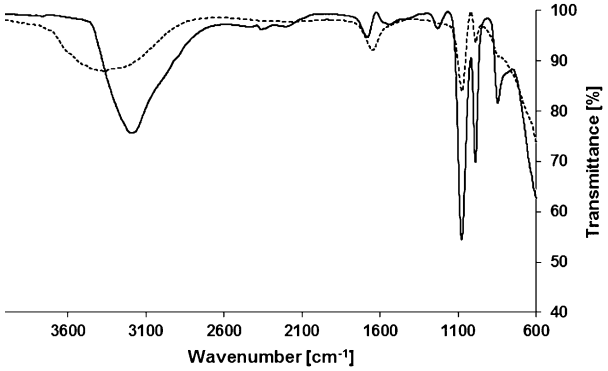

Figure 11. FTIR spectra of **2** (1 wt%) in 1 M sodium phosphate at pH 10 (dotted line = supersaturated solution; continuous line = hydrogel).

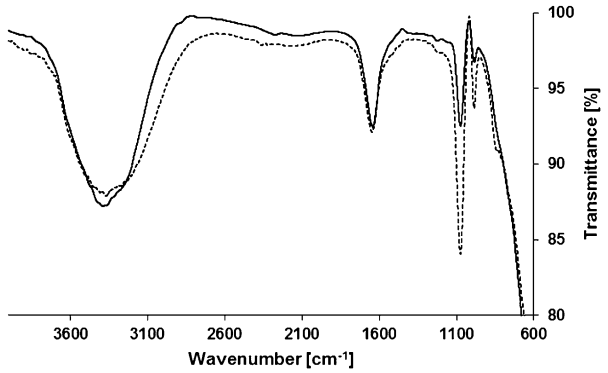

Figure 12. FTIR spectra of a supersaturated solution of **2** (1 wt%) at pH 10 in 1 M sodium phosphate (dotted line) and 1 M potassium phosphate (continuous line).

phosphate buffers reveals a significant difference in the intensities of the phosphate bands (Figure 12); the phosphate bands in potassium phosphate buffer turn out to be much weaker than in sodium phosphate buffer, which indicates that potassium significantly disturbs the self-assembly.

UV/Vis spectroscopy

Many reported LMWHGs depend on aromatic moieties such as phenylalanine or those with conjugated π systems such as fluorenyl, naphthyl, or pyrene groups.[23a,27] Because the gelation of **2** can only be observed under strongly basic conditions above the pK_{a1} of uracil (9.5),[28] it is likely that a single deprotonated species is necessary for decent self-aggregation. Some of the possible anionic tautomers of **2** (Figure 13) exhibit a more extensive π system (**2a**'' and **2b**''), which has often been observed to be important in the assembly of supramolecular hydrogels.

According to the literature, **2a** (λ_{max} = 260 nm) and **2b** (λ_{max} = 285 nm) show different absorption maxima, equally to the corresponding tautomers of unsubstituted uracil, and their ratio can be approximately estimated.[28,29] Therefore, we further investi-

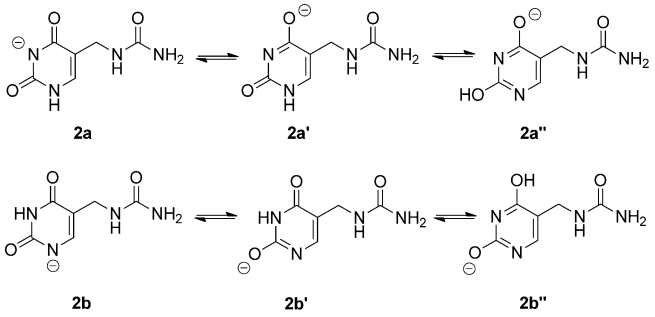

Figure 13. Anionic tautomers of **2**.

gated the tautomeric equilibria of **2** by UV/Vis spectroscopy. First, we were interested in the influence of the added phosphate salt. UV/Vis spectra were recorded in 1.0 M sodium phosphate and 1.0 M potassium phosphate buffers, as well as in sodium hydroxide solutions at pH 10. In aqueous sodium hydroxide solution at pH 10, both tautomers are present in about equal proportions.[28] However, the extinction coefficient of **2b** is higher than that of **2a**. Therefore the observed total spectrum of **2**, even though as a 1:1 mixture, shows a λ_{max} near 285 nm with a small shoulder at 265 nm (Figure 14, dotted line).[28,29]

In contrast, the UV spectrum of **2** in sodium phosphate buffer (Figure 14, continuous line) shows the opposite with a λ_{max} at 265 nm and a small shoulder at 285 nm, which indicates a significant shift of the equilibrium towards the 3-H-deprotonated species **2a**. This observation is in good agreement with Shapiro and Kang, who also reported that the 3-H-deprotonated uracil tautomer is favored in concentrated basic phosphate solutions.[28,29] When potassium phosphate buffer was used, the equilibrium shifts even more towards **2a** (Figure 14, dashed line). Because no hydrogels are formed under these conditions, this could imply that no single tautomer is important for the supramolecular aggregation, but the ratio between **2a** and **2b**. However, there was no evidence for the formation of **2a**'' or **2b**''.

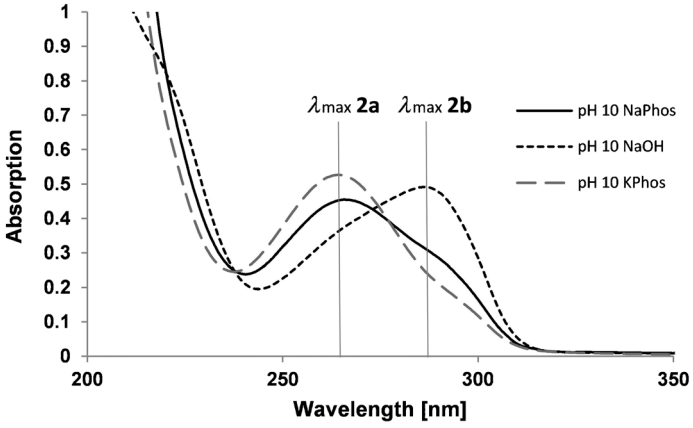

Figure 14. UV/Vis spectra of **2** at pH 10 in 0.1 mM sodium hydroxide (dotted line), 1.0 M sodium phosphate buffer (continuous line), and 1.0 M potassium phosphate buffer (dashed line).

Rheology

The mechanical gel strength was characterized by rheological strain sweep and frequency sweep experiments with different equivalents of phosphate. Figure 15 shows a strain sweep experiment in which the storage modulus G' and the loss modulus G'' are plotted against deformation. G' is typically three to ten times higher than G'', which demonstrates the viscoelastic behavior of the hydrogel.[27a,30] Furthermore, the high values of the storage modulus, more than 10^6 Pa, indicate a hydrogel with superior strength. We also investigated the influence of the phosphate ratio on gel strength (Figure 16). Addition of the minimal amount of 1 equiv of phosphate resulted in a relatively weak hydrogel with a G' of 10^2 Pa. By increasing the amount of phosphate to 1.5 equiv, which is the optimal ratio for the hydrogel, as identified by NMR titration experiments, G' increased dramatically up to 10^5 Pa. Further increases in phosphate led to an almost continuous increase in G'. The highest G'/G'' ratio is reached at 4 equiv of phosphate. This is in good agreement with our previous findings concerning a sudden decrease in MGC and a saturation effect at this ratio. In agreement with the MGC and titration experiments, there was no significant influence on rheological parameters when more than 8 equiv of phosphate were added.

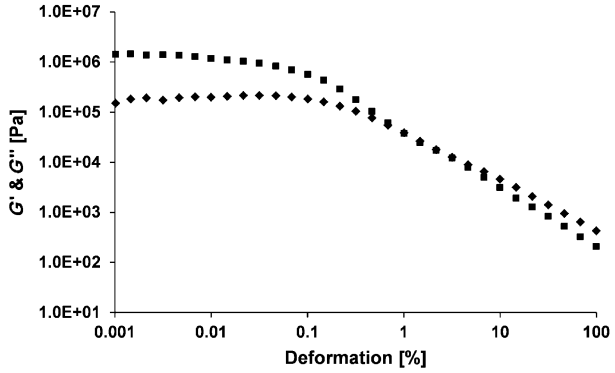

Figure 15. Rheological strain sweep experiment of a hydrogel of **2** (5 wt% + 4 equiv sodium phosphate) at pH 10.

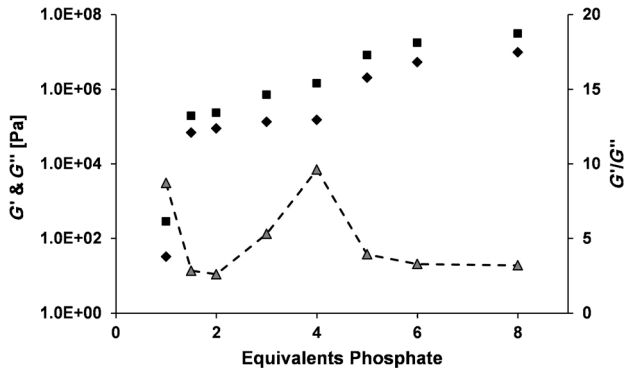

Figure 16. G' (black squares) and G'' (black diamonds) of a hydrogel containing 5 wt% of **2** and different equivalents of phosphate (left y axis) and G'/G'' ratio (grey triangles, right y axis) at 8 °C.

The hydrogel also showed impressive regeneration behavior; Figure 17 displays the results of the thixotropy/regeneration experiment. The hydrogel was allowed to mature for 30 min (until constant G' and G'' values were reached), then sheared for 30 s at 100% deformation to destroy the supramolecular network, and finally allowed to regenerate.

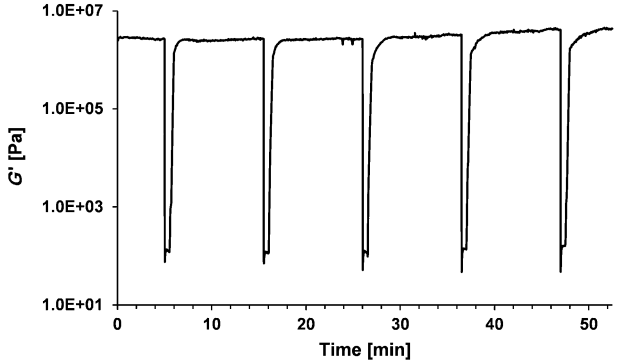

Figure 17. Rheological thixotropy/regeneration experiment performed on a hydrogel containing 5 wt% of **2** and 5 equiv of sodium phosphate at pH 10.

After only 1 min, complete regeneration of the hydrogel was observed. This process was repeated 10 times without any material fatigue, on the contrary, an increase in gel strength was observed, although the regeneration time increased slightly.

pH dependency

Because gelation could be triggered in the pH range from 10 to 12, we were also interested in the influence of pH on the fundamental material properties of the hydrogel. Therefore we conducted different rheological experiments to determine the dependence of gel strength, sol–gel transition temperature, and regeneration behavior of the hydrogel on pH (Table 2). We initially observed that the hydrogel becomes weaker as the pH is increased from 10 to 11, as reflected by a slight decrease in the storage modulus G'. Furthermore, the regeneration time after destruction of the gel by shear force increased by a factor of 10. In addition, the gel–sol transition temperature decreases with increasing pH.

Interestingly, when the pH was further increased to pH 12, at which complete deprotonation can be expected, the hydrogel becomes stronger than at pH 10, as indicated by the

Table 2. Variation of hydrogel parameters with pH.

pH	G' [10^6 Pa]	T_{gs} [°C]	Reg. time [min]
10	3.64	34.3	1.2
11	1.03	30.6	11.2
12	3.91	23.2	7.0

higher value of G'. In addition, the regeneration time decreased with respect to pH 11.

The change in the viscoelastic properties is also reflected in the macroscopic appearance and morphology of the corresponding xerogels. At pH 10 a turbid hydrogel is formed, whereas at pH 11 and 12 the hydrogels appear to be opaque. On a nanoscale, the almost parallel lamellae of the xerogel at pH 10 (Figure 18A) changed to a honeycomb-like morphology at pH 11 (Figure 18B). The xerogel at pH 12 (Figure 18C), on the other hand, shows a highly porous morphology with disordered lamella regions (see the Supporting Information for different magnifications).

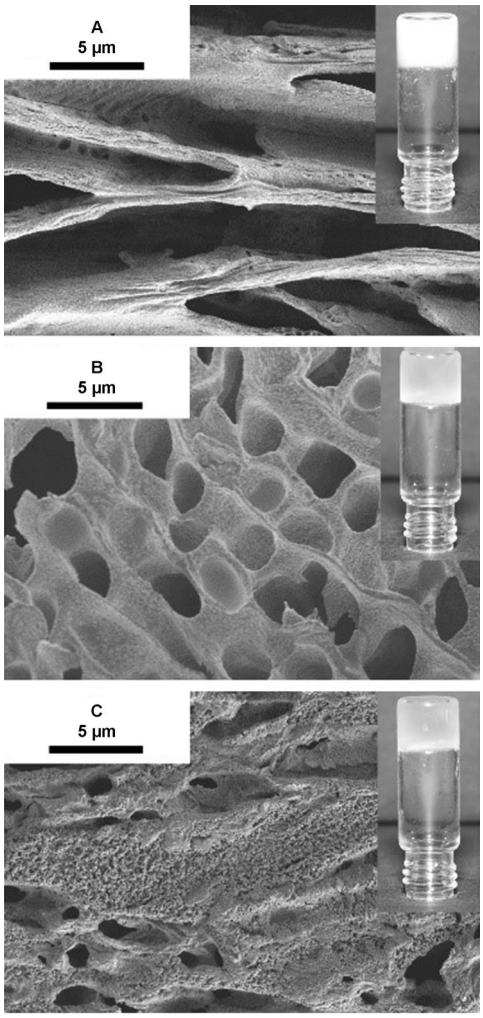

Figure 18. SEM images of xerogels of **2** (5 wt% of **2**+5 equiv phosphate) at A) pH 10, B) pH 11, and C) pH 12.

Conclusion

N-[(Uracil-5-yl)methyl]urea (**2**) represents not only a minimalistic pyrimidine-containing hydrogelator, but is also a rare example of a urea-based molecule, the self-assembly of which can be triggered by phosphate anions. Accordingly, this very simple hydrogelator is the lowest-molecular-weight hydrogelator comprising a nucleobase. In addition, **2** shows an impressive self-healing ability with a remarkably fast regeneration time and a high storage modulus of up to 10^7 Pa. Its stiffness, elasticity, gel–sol transition temperature, morphology, and regeneration ability are dramatically affected by simply varying the amount of phosphate salt added or the pH. Even though UV experiments revealed the importance of enol tautomerism for self-assembly and the ideal ratio for self-assembly between **2** and phosphate was found to be 1:1.5, as revealed by Job plot analysis, we have no detailed knowledge of the molecular structure of the hydrogel. This will form a part of future investigations.

Experimental Section

Materials

Unless otherwise stated, all chemicals were used as received from a commercial supplier. The water used for the preparation for the hydrogels and buffers was of Millipore Milli-Q grade.

Scanning electron microscopy

The hydrogel samples were prepared on aluminum sheets, lyophilized, and coated with a thin layer of platinum by using a Balzers SCD 050 sputter coater. A Zeiss DSM 940 scanning electron microscope was used to record the images of the xerogels with an accelerating voltage of 10 kV. For higher magnifications, the samples were prepared without metal coating and images were recorded on an Hitachi SU8030 scanning electron microscope using an accelerating voltage of 1 kV.

Transmission electron microscopy

TEM images were recorded with an Hitachi SU8030 scanning electron microscope in STEM mode at an accelerating voltage of 30 kV. The hydrogel samples were lyophilized and distributed onto a TEM grid (200 mesh copper grid) that was coated with carbon film.

NMR spectroscopy

^{1}H and ^{13}C NMR spectra of compounds **1** and **2** and ^{1}H NMR titration experiments were recorded on a Bruker Advance 400 MHz instrument in [D_6]DMSO. The ^{1}H chemical shifts are reported as δ (parts per million) relative to the quintet signal of DMSO at 2.50 ppm. The ^{13}C chemical shifts are reported as δ (parts per million) relative to the DMSO septet at 39.43 ppm. The following abbreviations have been used to describe splitting patterns: br = broad, s = singlet, d = doublet, t = triplet, q = quartet, qi = quintet, m = multiplet. Coupling constants J are given in Hz. ^{13}C NMR titration experiments were performed on a Bruker DRX-250 instrument in D_2O. Chemical shifts are reported as δ (parts per million) relative to the singlet signal arising from [2,2,3,3-D_4]3-(trimethylsilyl)propionic acid sodium salt at 0.0 ppm. ^{31}P MAS NMR spectra were recorded at 202 MHz on a Bruker AVII+500 NMR spectrometer with a 4 mm triple resonance HR/MAS probehead. The hydrogel samples were measured at 8 °C at spinning frequencies of 2.5 or 4.0 kHz.

FTIR spectroscopy

IR spectra were recorded with a Jasco FT/IR-4100 spectrometer. The corresponding buffers were used for background measurements of the hydrogels and supersaturated solutions.

UV/Vis spectroscopy

UV/Vis spectra were recorded with a Perkin–Elmer Lambda 2 UV/Vis spectrometer. The concentration of the samples was 0.08 mM and of the buffers was 1.0 M.

Rheology

Rheological measurements were carried out by using an Anton Paar Physica MCR 501 instrument. The geometry was plate–plate with a diameter of 25 mm and a 0.2 mm gap between the plates. The hydrogel samples were heated until complete dissolution, applied to the rheometer plate, and subsequently cooled to 8 °C after moving the stamp into the measuring position. For comparing strain sweep experiments with different amounts of phosphate, the samples were matured for about 30 min at 8 °C, until G' and G'' reached a constant level, and measured at 8 °C. For other experiments, the hydrogel samples were cooled to 8 °C for 10 min, subsequently heated to 20 °C, matured for another 20 min until G' and G'' reached a constant level, and measured at 20 °C. Strain sweep experiments were conducted with a constant angular frequency of 10 rad s^{-1} and frequency sweep experiments were undertaken with a constant deformation of 0.005%. The thixotropy/regeneration experiments were carried out by application of a continuous deformation of 0.005% for 5 min, followed by rupture of the gel at 100% deformation for 30 s. After complete rupture of the gel, as denoted by $G'' > G'$, gel recovery was observed at a constant deformation of 0.005%. The entire study was performed at a constant angular frequency of 10 rad s^{-1}.

Mass spectrometry

Mass spectra were recorded on a Finnigan MAT95 spectrometer. High-resolution mass spectra were recorded by using ESI method with a Bruker Daltonics Apex II FT-ICR mass analyzer.

Minimal gelator concentration (MGC)

MGCs were determined by means of the inverted vial test. Screw cap vials with a volume of 4.0 mL and sample volumes of 0.5 mL were used. The sample was heated until a clear solution was obtained and cooled for 10 min in an ice bath. The sample was defined as a hydrogel if no gravitational flow was observed upon inversion.

Synthesis of 5-(Hydroxymethyl)-2,4(1*H*,3*H*)-pyrimidinedione (1)

Uracil (10.00 g, 89.20 mmol) and paraformaldehyde (3.35 g, 111.50 mmol) were added to a 0.54 M aqueous solution of KOH (100 mL) and the reaction mixture was stirred at 55 °C for 72 h. The solvent was then removed under reduced pressure to one third volume, and the same volume of acetone was added. The precipitate was filtered, washed with acetone, and dried under vacuum. The pure product was obtained by recrystallization from water (10.78 g, 75.86 mmol, 85% yield). ^{1}H NMR (400 MHz, [D$_6$]DMSO): $\delta =$ 11.04 (br s, 1H, CON*H*CO), 10.70 (br s, 1H, CHN*H*), 7.24 (s, 1H, C*H*), 4.84 (br s, 1H, O*H*), 4.10 ppm (s, 2H, CH_2); ^{13}C{^{1}H} NMR (100 MHz, [D$_6$]DMSO): $\delta = 163.7$ (NH*C*OC), 151.3 (NH*C*NH), 138.0 (*C*H), 112.6 (*C*HC), 55.7 ppm (*C*H$_2$); MS (FAB, +): *m/z*: 142.0 $[M+H]^+$. The analytical data is in agreement with literature.[31]

Synthesis of *N*-[(Uracil-5-yl)methyl]urea (2)

Concentrated hydrochloric acid (2.89 mL, 35.18 mmol) was added to a solution of 1-hydroxymethyluracil (**1**; 1.00 g, 7.04 mmol) in water (25 mL) and the reaction mixture was slowly added dropwise to a stirred solution of urea (2.11 g, 35.18 mmol) in water (10 mL) at 80 °C. After complete addition, the mixture was stirred for 4 h at 80 °C and subsequently cooled in an ice bath. The precipitate was filtered, washed with water, and dried under vacuum to yield the pure product (1.06 g, 5.77 mmol, 82%). In some cases it was necessary to suspend the solid again in boiling water, filter whilst hot, and evaporate to yield the pure product. ^{1}H NMR (400 MHz, [D$_6$]DMSO): $\delta = 11.12$ (br s, 1H, CON*H*CO), 10.71 (br s, 1H, CHN*H*), 7.19 (s, 1H, C*H*), 6.11 (t, $^3J_{HH} = 6.0$ Hz, 1H, CH$_2$N*H*), 5.52 (s, 2H, NH_2), 3.74 ppm (d, $^3J_{HH} = 6.0$ Hz, 2H, CH_2); ^{13}C{^{1}H} NMR (100 MHz, [D$_6$]DMSO): $\delta = 164.2$ (NH*C*OC), 158.4 (NH*C*ONH$_2$), 151.1 (NH*C*NH), 138.5 (*C*H), 110.6 (*C*HC), 35.6 ppm (*C*H$_2$); FTIR (neat): 3445.2 (m), 3414.4 (m), 3013.2 (m), 2832.0 (s), 1708.6 (s), 1630.5 (vs), 1590.0 (vs), 1538.9 (vs), 1452.1 (s), 1436.7 (s), 1322.9 (m), 1245.8 (s), 1212.0 (s), 1123.3 (w), 1009.6 (w), 888.1 (s), 857.2 (s), 823.5 (s), 756.9 (s). 643.1 cm^{-1} (w); MS (HR-FTICR, +): *m/z* calcd for $[M+Na]^+$ 207.048861; found: 207.049027.

Acknowledgements

Financial support by the Baden-Württemberg Stiftung (Junior Professor Programm) and the Fonds der Chemischen Industrie (Sachkostenzuschuss and Ph. D. stipend to N.M.W.) is gratefully acknowledged. Elke Nadler and Prof. Tomas Chassé (Institut für Physikalische Chemie, Tübingen) are acknowledged for assistance with electron microscopy. Prof. Rolf Daniels (Institut für Pharmazeutische Technologie, Tübingen) is acknowledged for assistance with rheological measurements.

Keywords: gels · hydrogen bonds · nucleobases · self-assembly · urea

[1] J. W. Steed, *Chem. Soc. Rev.* **2010**, *39*, 3686–3699.
[2] a) L. Brunsveld, B. J. B. Folmer, E. W. Meijer, R. P. Sijbesma, *Chem. Rev.* **2001**, *101*, 4071–4097; b) O. Gronwald, E. Snip, S. Shinkai, *Curr. Opin. Colloid Interface Sci.* **2002**, *7*, 148–156; c) A. R. Hirst, D. K. Smith, *Chem. Eur. J.* **2005**, *11*, 5496–5508; d) J. A. Foster, M.-O. M. Piepenbrock, G. O. Lloyd, N. Clarke, J. A. K. Howard, J. W. Steed, *Nat. Chem.* **2010**, *2*, 1037–1043; e) J. W. Steed, *Chem. Commun.* **2011**, *47*, 1379–1383.
[3] a) T. Becker, C. Yong Goh, F. Jones, M. J. McIldowie, M. Mocerino, M. I. Ogden, *Chem. Commun.* **2008**, 3900–3902; b) M.-O. M. Piepenbrock, G. O. Lloyd, N. Clarke, J. W. Steed, *Chem. Rev.* **2010**, *110*, 1960–2004; c) J.-S. Shen, Q.-G. Cai, Y.-B. Jiang, H.-W. Zhang, *Chem. Commun.* **2010**, *46*, 6786–6788.
[4] S. R. Haines, R. G. Harrison, *Chem. Commun.* **2002**, 2846–2847.
[5] a) T. Naota, H. Koori, *J. Am. Chem. Soc.* **2005**, *127*, 9324–9325; b) K. Isozaki, H. Takaya, T. Naota, *Angew. Chem.* **2007**, *119*, 2913–2915; *Angew. Chem. Int. Ed.* **2007**, *46*, 2855–2857.
[6] a) S. Kume, K. Kuroiwa, N. Kimizuka, *Chem. Commun.* **2006**, 2442–2444; b) J. H. Kim, M. Seo, Y. J. Kim, S. Y. Kim, *Langmuir* **2009**, *25*, 1761–1766.
[7] a) M. George, R. G. Weiss, *Acc. Chem. Res.* **2006**, *39*, 489–497; b) A. R. Hirst, B. Escuder, J. F. Miravet, D. K. Smith, *Angew. Chem.* **2008**, *120*, 8122–8139; *Angew. Chem. Int. Ed.* **2008**, *47*, 8002–8018; c) A. Ajayaghosh, V. K. Praveen, C. Vijayakumar, *Chem. Soc. Rev.* **2008**, *37*, 109–122; d) S. Banerjee, R. K. Das, U. Maitra, *J. Mater. Chem.* **2009**, *19*, 6649–6687.
[8] a) K. Y. Lee, D. J. Mooney, *Chem. Rev.* **2001**, *101*, 1869–1880; b) T. Miyata, T. Uragami, K. Nakamae, *Adv. Drug Delivery Rev.* **2002**, *54*, 79–98; c) J. C. Tiller, *Angew. Chem.* **2003**, *115*, 3180–2183; *Angew. Chem. Int. Ed.* **2003**,

42, 3072 – 3075; d) S. Zhang, *Nat. Mater.* **2004**, *3*, 7 – 8; e) Y. Tang, C. L. Heaysman, S. Willis, A. L. Lewis, *Expert Opin. Drug Delivery* **2011**, *8*, 1141 – 1159.

[9] a) L. A. Estroff, A. D. Hamilton, *Chem. Rev.* **2004**, *104*, 1201 – 1216; b) T. Park, S. C. Zimmerman, *J. Am. Chem. Soc.* **2006**, *128*, 11582 – 11590; c) C. Yan, D. J. Pochan, *Chem. Soc. Rev.* **2010**, *39*, 3528 – 3540; d) E. K. Johnson, D. J. Adams, P. J. Cameron, *J. Mater. Chem.* **2011**, *21*, 2024 – 2027; e) L. E. Buerkle, S. J. Rowan, *Chem. Soc. Rev.* **2012**, *41*, 6089 – 6102; f) A. Noro, M. Hayashi, Y. Matsushita, *Soft Matter* **2012**, *8*, 6416 – 6429; g) H. Wang, Z. Yang, *Nanoscale* **2012**, *4*, 5259 – 5267; h) H. Wang, Z. Yang, D. J. Adams, *Mater. Today* **2012**, *15*, 500 – 507; i) J. Raeburn, A. Zamith Cardoso, D. J. Adams, *Chem. Soc. Rev.* **2013**, *42*, 5143 – 5156.

[10] P. K. Vemula, G. John, *Chem. Commun.* **2006**, 2218 – 2220.

[11] D. K. Kumar, D. A. Jose, A. Das, P. Dastidar, *Chem. Commun.* **2005**, 4059 – 4061.

[12] J.-U. Kim, D. Schollmeyer, M. Brehmer, R. Zentel, *J. Colloid Interface Sci.* **2011**, *357*, 428 – 433.

[13] S. M. Park, Y. S. Lee, B. H. Kim, *Chem. Commun.* **2003**, 2912 – 2913.

[14] X. Li, Y. Kuang, B. Xu, *Soft Matter* **2012**, *8*, 2801 – 2806.

[15] a) G. Wang, A. D. Hamilton, *Chem. Commun.* **2003**, 310 – 311; b) L. A. Estroff, L. Addadi, S. Weiner, A. D. Hamilton, *Org. Biomol. Chem.* **2004**, *2*, 137 – 141; c) M. de Loos, A. Friggeri, J. van Esch, R. M. Kellogg, B. L. Feringa, *Org. Biomol. Chem.* **2005**, *3*, 1631 – 1639; d) M. Ávalos, R. Babiano, P. Cintas, A. Gómez-Carretero, J. L. Jiménez, M. Lozano, A. L. Ortiz, J. C. Palacios, A. Pinazo, *Chem. Eur. J.* **2008**, *14*, 5656 – 5669; e) F. Rodríguez-Llansola, B. Escuder, J. F. Miravet, D. Hermida-Merino, I. W. Hamley, C. J. Cardin, W. Hayes, *Chem. Commun.* **2010**, *46*, 7960 – 7962; f) G. O. Lloyd, J. W. Steed, *Soft Matter* **2011**, *7*, 75 – 84; g) M. Yamanaka, N. Haraya, S. Yamamichi, *Chem. Asian J.* **2011**, *6*, 1022 – 1025; h) F. Rodríguez-Llansola, D. Hermida-Merino, B. Nieto-Ortega, F. J. Ramirez, J. T. L. Navarrete, J. Casado, I. W. Hamley, B. Escuder, W. Hayes, J. F. Miravet, *Chem. Eur. J.* **2012**, *18*, 14725 – 14731; i) Y. Jinno, M. Yamanaka, *Chem. Asian J.* **2012**, *7*, 1768 – 1771; j) D. Higashi, M. Yoshida, M. Yamanaka, *Chem. Asian J.* **2013**, *8*, 2584 – 2587; k) K. Liu, J. W. Steed, *Soft Matter* **2013**, *9*, 11699 – 11705; l) M. Yamanaka, *J. Inclusion Phenom. Macrocyclic Chem.* **2013**, *77*, 33 – 48; m) J. A. Foster, R. M. Edkins, G. J. Cameron, N. Colgin, K. Fucke, S. Ridgeway, A. G. Crawford, T. B. Marder, A. Beeby, S. L. Cobb, J. W. Steed, *Chem. Eur. J.* **2014**, *20*, 279 – 291.

[16] a) R. Iwaura, K. Yoshida, M. Masuda, K. Yase, T. Shimizu, *Chem. Mater.* **2002**, *14*, 3047 – 3053; b) L. Moreau, P. Barthélémy, M. El Maataoui, M. W. Grinstaff, *J. Am. Chem. Soc.* **2004**, *126*, 7533 – 7539; c) X. Li, X. Du, Y. Gao, J. Shi, Y. Kuang, B. Xu, *Soft Matter* **2012**, *8*, 7402 – 7407; d) R. Iwaura, M. Ohnishi-Kameyama, *Chem. Commun.* **2012**, *48*, 6633 – 6635.

[17] A. J. Kleinsmann, B. J. Nachtsheim, *Chem. Commun.* **2013**, *49*, 7818 – 7820.

[18] M. D. Segarra-Maset, V. J. Nebot, J. F. Miravet, B. Escuder, *Chem. Soc. Rev.* **2013**, *42*, 7086 – 7098.

[19] G. O. Lloyd, M.-O. M. Piepenbrock, J. A. Foster, N. Clarke, J. W. Steed, *Soft Matter* **2012**, *8*, 204 – 216.

[20] T. P. Johnston, G. S. McCaleb, J. A. Montgomery, *J. Med. Chem.* **1963**, *6*, 669 – 681.

[21] R. E. Cline, R. M. Fink, K. Fink, *J. Am. Chem. Soc.* **1959**, *81*, 2521 – 2527.

[22] M. Suzuki, M. Yumoto, H. Shirai, K. Hanabusa, *Org. Biomol. Chem.* **2005**, *3*, 3073 – 3078.

[23] a) Z. Yang, B. Xu, *J. Mater. Chem.* **2007**, *17*, 2385 – 2393; b) P. K. Sukul, S. Malik, *Soft Matter* **2011**, *7*, 4234 – 4241; c) Y. Gao, M. J. C. Long, J. Shi, L. Hedstrom, B. Xu, *Chem. Commun.* **2012**, *48*, 8404 – 8406.

[24] a) Y. Li, J. Liu, G. Du, H. Yan, H. Wang, H. Zhang, W. An, W. Zhao, T. Sun, F. Xin, L. Kong, Y. Li, A. Hao, J. Hao, *J. Phys. Chem. B* **2010**, *114*, 10321 – 10326; b) A. Tripathi, P. S. Pandey, *Tetrahedron Lett.* **2011**, *52*, 3558 – 3560; c) I. Kapoor, E.-M. Schon, J. Bachl, D. Kuhbeck, C. Cativiela, S. Saha, R. Banerjee, S. Roelens, J. J. Marrero-Tellado, D. D. Diaz, *Soft Matter* **2012**, *8*, 3446 – 3456.

[25] F. A. Miller, C. H. Wilkins, *Anal. Chem.* **1952**, *24*, 1253 – 1294.

[26] B. Roy, A. Saha, A. Esterrani, A. K. Nandi, *Soft Matter* **2010**, *6*, 3337 – 3345.

[27] a) A. M. Smith, R. J. Williams, C. Tang, P. Coppo, R. F. Collins, M. L. Turner, A. Saiani, R. V. Ulijn, *Adv. Mater.* **2008**, *20*, 37 – 41; b) T. Kar, S. K. Mandal, P. K. Das, *Chem. Eur. J.* **2011**, *17*, 14952 – 14961; c) J. Nanda, A. Biswas, A. Banerjee, *Soft Matter* **2013**, *9*, 4198 – 4208.

[28] R. Shapiro, S. Kang, *Biochim. Biophys. Acta* **1971**, *232*, 1 – 4.

[29] a) N. Iza, M. Gil, J. Morcillo, *J. Mol. Struct.* **1988**, *175*, 31 – 36; b) B. E. Billinghurst, S. A. Oladepo, G. R. Loppnow, *J. Phys. Chem. B* **2009**, *113*, 7392 – 7397.

[30] a) B. Adhikari, J. Nanda, A. Banerjee, *Soft Matter* **2011**, *7*, 8913 – 8922; b) J. Nanda, A. Banerjee, *Soft Matter* **2012**, *8*, 3380 – 3386.

[31] L. Bérillon, R. Wagner, P. Knochel, *J. Org. Chem.* **1998**, *63*, 9117 – 9121.

Received: April 2, 2014
Published online on July 7, 2014